Chapter 3

Bifurcation Makes a Wave Resonant Solid-State Gyro Be Stable

Svetlana Pavlovna Nikitenkova and
Dmitry Anatolyevich Kovriguine

Additional information is available at the end of the chapter

http://dx.doi.org/10.5772/intechopen.71726

Abstract

A golf ball having special dimples flies better than an analogous smoothed one. A surprise is that there is a range of Reynolds numbers for which the turbulent drag is somewhat less than that in the laminar case. Analogies always meet together and are accomplished themselves in the physics. We have traced an effect similar to the above mentioned in the area of solid mechanics when the nonlinear system passes through a sequence of bifurcations. In mechanical engineering, the role of such a system can play a solid-state wave gyro entering the family of MEMS/NEMS. It is known that a circular Foucault pendulum can serve as an angular sensor. Standing waves in a thin-walled elastic axisymmetric resonator of a solid-state wave gyro, mounted on a rotating platform, can also detect a rotation rate. Because there are no typical mechanical parts there, such wave sensors have advantages for long-term space missions. However, to maintain the functionality and sensitivity of a wave gyro in practice, the driving of standing waves requires a sophisticated feedback control. Nonetheless, we have demonstrated that such a gyro can operate without any feedback at the expense of the natural nonlinearity of the resonator in a postbifurcation regime.

Keywords: wave solid-state gyro, Foucault pendulum, spring pendulum, bifurcation, stability

1. Introduction

It is well known that the aerodynamic drag is proportional, first of all, to the kinetic energy of a flow. Moreover, the drag depends on a lot of other almost uncontrolled factors such as the shape, size, inclination of the object in the flow, etc. Implicitly, all these are accumulated all together in the following formula for the hydrodynamic resistance: $c_d \rho F V 2/2$, where ρ is the density of a fluid or gas, V is the velocity of a flow, F denotes an effective area of the object, c_d

stands for the so-called drag coefficient being a dimensionless characteristic function versus the Reynolds number. Recall that the Reynolds number is usually defined as Vl/ν, where l is an effective length, ν is the kinematic viscosity coefficient. The function c_d is respective for all the uncontrolled points accompanying the interaction between the body and the flow. This function can be recorded experimentally using a wind tube. Experimental results obtained are used to evaluate the drag on other similar objects. In particular, the similarity by the Reynolds number ensures a correct description of viscous motions. Notice that the drag coefficient is nearly a constant in a wide range of Reynolds numbers in most practical cases. As long as the flow velocity would increase, the Reynolds number also increases. It is well known that in a slow flow, the viscosity can be neglected in practice. In this case, one can observe almost an ideal flow with no boundary layer near the surface. Therefore, there is almost no resistance to the motion in accordance with well-known d'Alembert paradox. As the velocity increases further, the drag becomes non-zero as a result of vortex generation. Then, these vortexes oscillate to produce the so-called Kármán vortex street, while the drag increases gradually together with the flow speed. At even higher velocity, the boundary layer turns into a chaotic turbulent flow. It is natural to expect that the turbulent drag would be higher than that in the laminar flow case. Nonetheless, a surprise is that there is a range of Reynolds numbers for which the turbulent drag is somewhat less than that in the laminar case. It is observed experimentally that a roughened cylinder or a ball will pass the turbulent flow at a lower Reynolds number than a smooth cylinder or a ball. At first sight, this results in a rather paradoxical result: there is a small range of Reynolds numbers for which the drag of a roughened body is less than the drag of a smooth body of the same size. For a good example, we can recall a golf ball having special dimples. Indeed, the golf with those dimples flies better than an analogous smoothed one [1].

Physical analogies meet together and are accomplished themselves in most applications. Can we find out an effect similar to the abovementioned dimpled ball that flies better in the area of solid mechanics? We know that the hydrodynamic drag evolves throughout the sequence of bifurcations. But any bifurcation is inherent in nonlinear systems. Therefore, our study should deal with nonlinear mechanical systems. In mechanical engineering, the machines, sensors, and other useful devices are of interest. One of them is a solid-state wave gyro from the family of microelectromechanical system/nanoelectromechanical system (MEMS/NEMS) devices. Let us briefly touch some key points of this topic.

In the nineteenth century, people held no doubt that the Earth is turning about its axis. However, there were no direct proofs. For this reason, Léon Foucault had managed in 1851 his famous experiment with the giant pendulum. The heart of his experiment is the inertia of the pendulum or the resistance to change the motion. This means that the swing plane remains to be fixed in Newton's absolute frame of references; moreover, this evidence can be traced with the naked eye due to the slow clockwise veering since the Earth rotates anti-clockwise. However, Foucault's pendulum has one essential flaw, namely the dependence on the latitude and its giant size suppressing the energy dissipation for a while. That is why, in 1852, though an idea, we should note, was not new, Foucault produced a compact and convenient gyroscopic setup based on the immobility of the axis of a rotating mass. It was a prototype of a

http://dx.doi.org/10.5772/intechopen.71726

conventional gyro providing needed horizons at sea and then in the air. The irony of fate, when the twentieth century was ending, the old idea came back to use a Foucault-pendulum-based device as a high precision gyroscope, although, in the other role of a thin axisymmetric solid-state resonator, associated with satellite guidance systems intended for long-term missions extending up to 15 years [6].

In 1890, Bryan demonstrated that the revolving of the standing wave nodes records effectively the rotation of the elastic resonator, as equally as a material point tends to conserve the spatial position in Newton's space. This evidence was not so new. Yet before Bryan's experiments, it was well known that the plane of transverse vibration of a straight wire will remain fixed in space instead of turning, though the wire rotates slowly about its axis during oscillations. Bryan noticed that when the vibrating body is such as a bell, rotation about its axis will produce an intermediate effect: the nodal meridians revolve with angular velocity less than that of the resonator that exhibits a new finding which yet nothing is easier than to be verified experimentally. He selected a champagne glass, then struck it to get a pure tone and when the glass turns around, Bryan heard sound beats demonstrating that the nodal meridians do not remain fixed in Newton's absolute space. He evaluated that the nodal angular velocity is about 3/5 of this almost hemispherical resonator [7]. Although, only in the second half of the twentieth century, Bryan's effect gets a wide extent turning into a concept of a prototype of an angle sensor that possesses a lot of advantages compared with a conventional gyro because its core is a monolith [8–10]. Moreover, if the power of the wave gyro is lost for a short time, the resonator conserves the angular rate, so that when the power returns, the gyro need not be reinstalled, etc., unlike, for instance, optical gyroscopes.

Let us now recall some mathematical aspects of the problem along the natural evolution of ideas. The role of the most simple mechanical system, appearing as an abstract oscillatory gyro *in vitro*, can play a circular Foucault pendulum. The corresponding mathematical model can be given by the following two differential equations:

$$\begin{aligned} &\ddot{x} - 2\Omega \quad \sin\varphi\dot{x} + \omega^2 x = 0; \\ &\ddot{y} + 2\Omega \quad \sin\varphi\dot{y} + \omega^2 y = -r\Omega^2 \sin\varphi\cos\varphi, \end{aligned} \tag{1}$$

where φ defines the latitude of geographical place; Ω is the Earth's angular velocity in absolute value; r is the Earth's radius plus a distance from the point where the pendulum is suspended. It is supposed that Earth rotates about the axis z. Here, $x(t)$ and $y(t)$ denote the pair of projections of infinitesimal oscillations of the bob, weight mg, in the rotating Cartesian frame of references(O, x, y, z). The origin O belongs to the Earth's center while the plane (O, x, z) passes through both poles. For operating such a gyro *in vita*, the pendulum should be excited to vibrate. Moreover, the amplitude of oscillations has to be maintained on some sensitive level because of energy dissipation. The presence of damping requires permanently pumping the energy into these oscillations by external forces for a permanent operating.

Almost a half century later, Bryan has derived his equation describing two similar vibration forms which, traveling toward a thin rotating ring, produce phenomena of beats, and which, in the case of high-frequency oscillations like those of sound, can detect effects of slow rotation about the sensitivity axis:

$$v_{t,t} - v_{\theta,\theta,t,t} - 4\omega v_{\theta,t} + (\omega^2 - \mu)v_{\theta,\theta} + \frac{T(2v_{\theta,\theta} + v_{\theta,\theta,\theta,\theta})}{\sigma a^2} = \frac{\beta(v_{\theta,\theta,\theta,\theta,\theta,\theta} + 2v_{\theta,\theta,t,t} + v_{\theta,\theta})}{\sigma a^4}. \tag{2}$$

Here, $v = v(\theta, t)$ and $w(\theta, t)$ are the tangential and radial components of displacements measured in the rotating polar frame of references; $(a + w, \theta)$, at time t. The symbol ω denotes the angular rate; a is the radius of the ring; σ is mass density; $T = \sigma a^2(\omega^2 - \mu)$ stands for an attractive force μ, times the distance, directed toward the axis. We can consider this model of the circular ring as a prototype of a solid-state wave gyro to trace the precession of the flexural standing wave *in vacuo*, that is, in the absence of damping. However, the energy dissipation always presents in nature. Therefore, this system requires some external feedback control to supply the wave motion. The principal parametric resonance is a good way to excite such a gyro by driving the axisymmetric tension T. Nonetheless, some feedback is in need since the parametrically excited oscillations are always unstable either in the presence or in the absence of damping [8]. To maintain the functionality as well as the sensitivity of a conventional wave gyro in practice, the driving of standing waves requires a sophisticated feedback control to eliminate the unstable oscillations caused by their parametric excitation. Therefore, such a kind of wave excitation looks as not quite satisfactory from the viewpoint of actuation, driving or stability properties. Since the linear theory is not able to achieve the desired goal, it is necessary to look for other theoretical tools within the nonlinear wave dynamics. Our thought is to use the exclusive property of the axisymmetric mode of the ring to control the amplitude of flexural waves in the gyro in the presence of energy dissipation, just to use this one as a sort of catalysator in the dynamical process. This chapter demonstrates that when both the primary resonant pumping over the axisymmetric mode and the principal parametric resonant excitation are combined, such a gyro can operate without any feedback, just at the expense of the natural nonlinearity of the resonator in a post-bifurcation regime.

2. Spring pendulum

Before all the theoretical approaches related to a wave resonant solid-state gyro, it may be of place to consider a most simple mechanical system which behaves analogously and contains no excess detail, in order to explain from first principles why the nonlinearity stabilizes unstable parametric oscillations, at the expense of resonance experienced in the mechanical system. The best candidate seems to be a spring pendulum.

Therefore, let us consider a pendulum swinging in a plane and consisting of a bob of mass m attached to a spring with the stiffness k and of the natural length l. Under the Earth gravity, the equilibrium length of the pendulum becomes $l + \Delta$, where $\Delta = mg/k$ denotes the spring elongation. After introducing the time-dependent radial coordinate $r(t)$, perpendicularly to the pivot of the spring, and the angle $\theta(t)$ between the spring and the vertical, the equations governing the motion can be derived easily by using the following Lagrangian function:

$$\mathcal{L} = m\left[\dot{r}^2 + (l+r)^2\dot{\theta}^2 - \left(\dot{r}^2 + (l+r)^2\dot{\theta}^2\right)/2\right] + kr^2/2 + mg[(l+r)1 - \cos\theta - r]. \tag{3}$$

Alternatively, we may follow the Hamiltonian approach:

$$\mathcal{H} = \frac{p_1^2}{m} + \frac{p_2^2}{m\left(l+q_1\right)^2} - \frac{1}{2m}\left(\frac{p_1^2}{m^2} + \frac{p_2^2}{\left(l+q_1\right)^2 m^2}\right) + \frac{kq_1^2}{2} + mg\left(\left(l+q_1\right)\left(1-\cos q_2\right) - q_1\right), \tag{4}$$

and then writing the following set of Hamiltonian equations:

$$\begin{aligned} &\dot{q}_1 = \frac{p_1}{m}; \quad \dot{q}_2 = \frac{p_2}{m}\left(l+\Delta+q_1\right)^{-2}; \\ &\dot{p}_1 = \frac{p_2^2}{m}\left(l+\Delta+q_1\right)^{-3} - kq_1 + mg\left(\cos q_2 - 1\right); \\ &\dot{p}_2 = -mg\left(l+\Delta+q_1\right)\sin q_2, \end{aligned} \tag{5}$$

where $q_1 = r$, $q_2 = \theta$, $p_1 = m\dot{r}$, $p_2 = m(l+r)^2\dot{\theta}$ are the canonical coordinates. For further preparations, it is convenient to pass from the physical coordinates to dimensionless variables: $t = \tau/\Omega_1$; $p_1 = lm\Omega_1 z_3$; $p_2 = l^2 m\left(\Omega_1^2 + \Omega_2^2\right)^2 z_4/\Omega_1^3$; $q_1 = lz_1$; $q_2 = z_2$, where $\Omega_1 = \sqrt{k/m}$ and $\Omega_2 = \sqrt{g/l}$ denote the natural radial and angular frequencies of the pendulum with an inextensible thread at small oscillations. Notice that the angular frequency would be somewhat lower in the case of extensible thread, namely $\nu = \Omega_2/\sqrt{\Omega_1^2 + \Omega_2^2}$. In the new dimensionless variables, equations of infinitesimal oscillations would read

$$\begin{aligned} &\frac{dz_1}{d\tau} = z_3; \quad \frac{dz_2}{d\tau} = z_4; \\ &\frac{dz_3}{d\tau} = -z_1; \quad \frac{dz_4}{d\tau} = -\nu^2 z_2. \end{aligned} \tag{6}$$

Let us now consider small-but-finite oscillations of the pendulum. In this case, the general solution to the set (6) can be represented as follows:

$$\begin{cases} z_1(\tau) = -\mu A_1(T)\cos\ \left(\varphi_1(T) + \tau\right); \\ z_2(\tau) = -\mu\ A_2(T)\cos\ \left(\nu\tau + \varphi_2(T)\right)/\nu; \\ z_3(\tau) = \mu A_1(T)\sin\ \left(\varphi_1(T) + \tau\right); \\ z_4(\tau) = \mu A_2(T)\sin\ \left(\nu\tau + \varphi_2(T)\right) \end{cases} \tag{7}$$

to look for solutions to Eq. (5) with unknown amplitudes A_i and phases φ_i slowly evolving in the new slow time $T = \mu\tau$, where μ is arbitrary small-scaling parameter. The substitution from Eq. (7) into Eq. (5), and ordering in μ, yields the following set of first-order approximation evolution equations:

$$\begin{aligned} &\frac{dA_1}{dT} = -\frac{A_2^2}{2}\sin\Phi; \\ &\frac{dA_2}{dT} = \frac{9A_2A_1}{32}\sin\Phi; \\ &\frac{d\Phi}{dT} = \left(\frac{9A_1}{16} - \frac{2A_2^2}{A_1}\right)\cos\Phi, \end{aligned} \tag{8}$$

under the one assumption that the following integer-valued ratio between the frequencies, manifesting the primary parametric resonance, that is, $1:\nu=1:2$, takes place. Notice that the set (8) contains the so-called generalized phase $\Phi(T)=\varphi_1(T)-2\varphi_2(T)$, as the unknown variable. The set (8) is of Hamiltonian structure. So, the related average Hamiltonian function reads

$$A_2^2(T)A_1(T)\cos\Phi(T)=A_2^2(0)A_1(0). \tag{9}$$

Moreover, Eq. (8) posses one more additional integral of motion:

$$\mathcal{E}=\frac{9{A_1}^2}{32}+\frac{{A_2}^2}{2}, \tag{10}$$

where $\mathcal{E}=9A_1^2(0)/32+A_2^2(0)/2$ is the average kinetic energy of the pendulum defined at the initial instant of time. These two integrals, Eqs. (9) and (10), allow us to integrate the set (8) analytically in terms of Jacobi elliptic functions [3].

Let us now refer to the damped forced motion of the pendulum. In this case, equations governing the motion (5) can be easily modified to the following form:

$$\begin{aligned}
&\dot{q}_1=\frac{p_1}{m};\quad \dot{q}_2=\frac{p_2}{m}\left(l+\Delta+q_1\right)^{-2};\\
&\dot{p}_1=\frac{p_2^2}{m}\left(l+\Delta+q_1\right)^{-3}-kq_1+mg\left(\cos q_2-1\right)-2\mu\delta p_1-\mu F\cos\left(\Omega_1 t+\psi_1\right);\\
&\dot{p}_2=-mg\left(l+\Delta+q_1\right)\sin q_2-2\mu\delta p_2,
\end{aligned} \tag{11}$$

where δ is the viscous drag coefficient; F is the amplitude of an external harmonic force acting at the resonant frequency of free radial oscillations of the pendulum. We can utilize the same anzats (7) to derive the truncated set of modulation equation for slowly varying amplitudes and phases. Small parameter μ emphasizes that both the damping and forcing are small but finite. After the substitution from Eq. (7) into Eq. (11), and ordering in μ, the first-order approximation evolution equations describing the resonant excitation of the pendulum over the radial mode can be written as

$$\begin{aligned}
&\frac{dA_1}{dT}=-A_2^2\sin\Phi/2+G-\Lambda A_1;\\
&\frac{dA_2}{dT}=\frac{9A_2A_1\sin\Phi}{32}-\Lambda A_2;\\
&\frac{d\Phi}{dT}=-\left(\frac{A_2^2}{2A_1}+\frac{9A_1}{16}\right)\cos\Phi.
\end{aligned} \tag{12}$$

These equations take in a natural manner into account the so-called triad-angle locking phenomenon described in [2], when both the phase of external force and the phase of radial oscillations have to be coupled, that is, $-\varphi_1(T)+\psi_1=\pi/2$, accordingly the phase matching conditions. Notice that the parameter $G=F/6\text{mg}$, entering Eq. (12), is interpreted as the dimensionless force, while $\Lambda=\delta/\Omega_1$ stands for the dimensionless drag coefficient.

In the case of stationary motion, when the amplitudes are constants, Eq. (12) produces the following algebraic set of equations:

http://dx.doi.org/10.5772/intechopen.71726

$$-A_2^2/2 + G - \Lambda A_1 = 0; \quad \frac{9A_2A_1}{32} - \Lambda A_2 = 0; \quad \Phi(T) = \pi/2, \tag{13}$$

having the following solutions:

$$A_1 = \frac{G}{\Lambda}, A_2 = 0, \quad \text{when } K \leq \frac{32\Lambda^2}{9}; \tag{14}$$

and

$$A_1 = \frac{32\Lambda}{9}, A_2 = \sqrt{18G - 64\Lambda^2}/3, \quad \text{as } K > \frac{32\Lambda^2}{9}. \tag{15}$$

These solutions, Eqs. (14) and (15), are plotted in **Figure 1**. As we can see, the dimensionless parameter K plays the role of control parameter governing the bifurcation of the system. The stationary solution (14) near the bifurcation point $\overline{K} = 32\Lambda^2/9$ becomes unstable and gives way to the new stationary steady state (15).

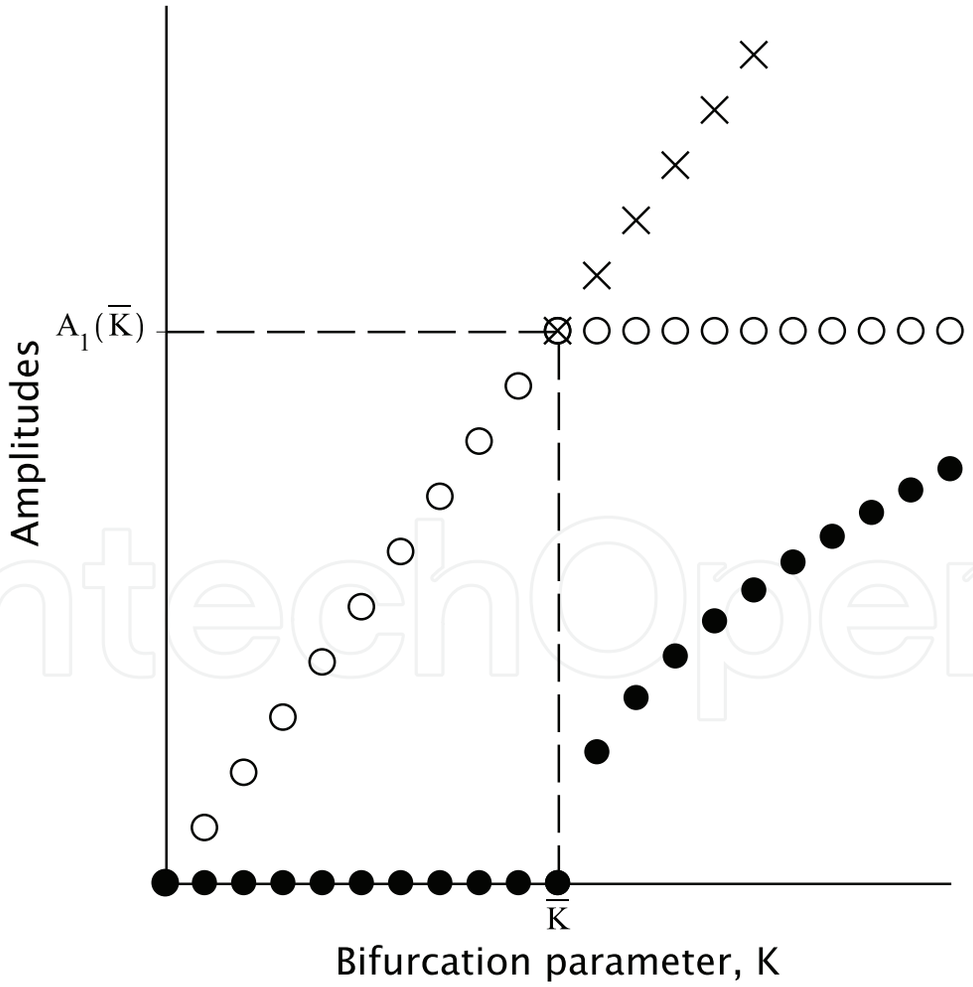

Figure 1. Bifurcation diagram—Amplitudes of radial and angular modes versus control parameter K. Solid circles refer to stable angular oscillations, circles mark stable radial oscillations. Crosses denote unstable radial mode. Change in the stability takes place near the bifurcation point $\overline{K}$ (parameter $\Lambda = 3/8\sqrt{2}$ has been scaled arbitrary for the best view).

To examine the stability properties without any excess mathematical preparations, let us analyze the power of drag forces using the energy balance resulted from the set (12):

$$\frac{d}{dT}\left(\frac{9A_1^2}{16}+A_2^2\right)=-\Lambda\left(\frac{9A_1^2}{16}+A_2^2\right)+\frac{9GA_1}{16}. \tag{16}$$

For the stationary orbits, the left-hand term of this equation is zero. Since the right-hand term, representing changes of the average kinetic energy in time, is also zero, then the power of drag forces should be, in turn, proportional to the kinetic energy with a negative sign. The diagram of the average kinetic energy as the function of control parameter K is shown in **Figure 2**. As we can see, the power of drag forces reduces after the bifurcation under the same external harmonic excitation. This means stability.

Let us now refer to the original Eq. (11) to verify results yielded by the modulation theory. To plot the numerical results, we have used the following transform: $t=\tau\sqrt{m/k}$; $p_1(t)=lm\sqrt{k/m}z_3(\tau)$; $p_2(t)=m\sqrt{k/m}(mg+lk)^2z_4(\tau)/k^2$; $q_1(t)=lz_1(\tau)$; $q_2(t)=z_2(\tau)$, from the physical to dimensionless variables. The numerical parameters of the system are chosen by us as

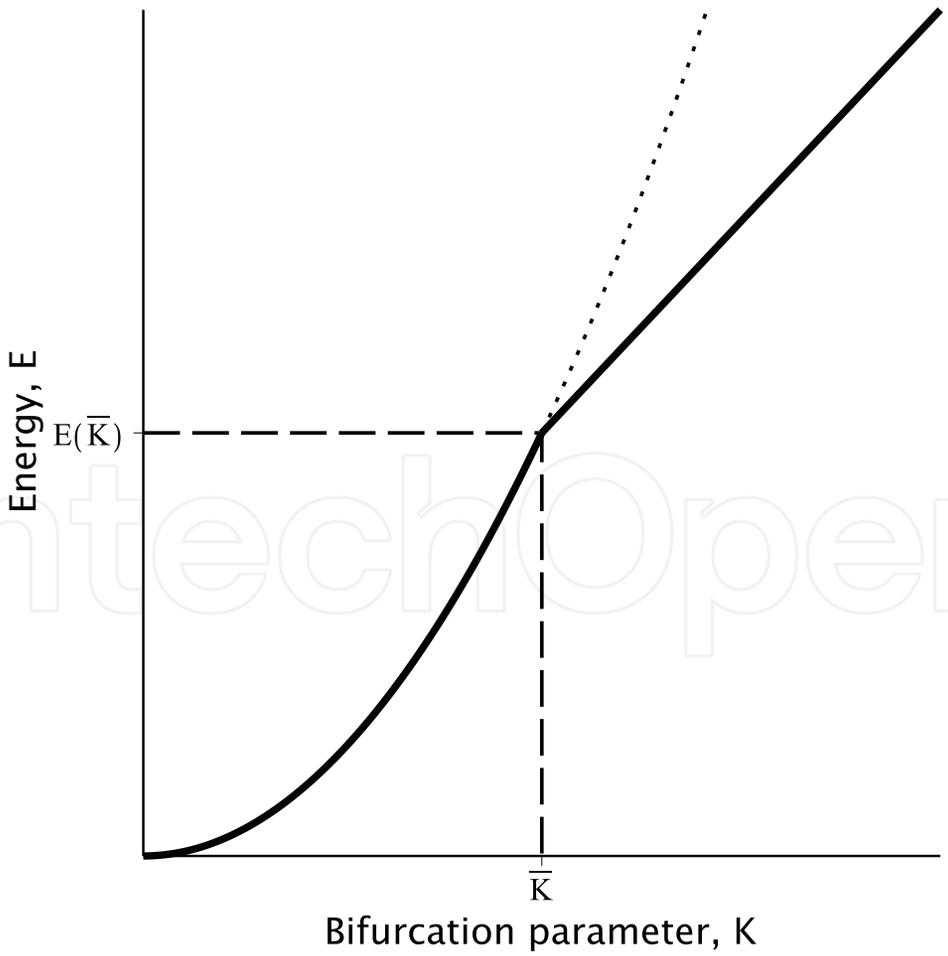

Figure 2. Bifurcation diagram—Average kinetic energy versus control parameter K. Solid lines refer to stable oscillations while dotted line marks unstable regime of oscillations. Parameter Λ is the same as in **Figure 1**.

follows: $F = 1.0\,\mathrm{N}$; $\beta = 0.01\,\mathrm{kg/s}$; $\delta = 0.01\,\mathrm{s}^{-1}$; $g = 9.8\,\mathrm{m/s}^2$; $k = 29.40\,\mathrm{kg/s}^2$; $l = 1.0\,\mathrm{m}$; $m = 1.0\,\mathrm{kg}$.

Since we are studying a damped forced motion, the initial conditions to the governing equations rewritten in terms of either the physical or the dimensionless variables $z_i(\tau)$ cannot play any role at large times, though we have decided to start in our calculations from the static equilibrium point. **Figure 3(a)** displays the time history of the radial coordinate of the system governed by Eq. (11), rewritten in new dimensionless variables $z_i(\tau)$, while the evolution of the angular oscillations is shown in **Figure 3(b)**. **Figure 4** displays a typical Lissajous curve that appears on (z_1, z_2) cross section of the four-dimensional phase space for the fully developed stationary state. **Figure 5** shows individual cross sections related to the radial and angular vibrations in the developed stationary regime of oscillations. Finally, **Figure 6** exhibits the evolution of the Hamiltonian function (4) or the energy of the system (11) in comparison with that one where the angular coordinate is fixed to zero but the force excitation remains the same. Notice that if the angular coordinate is fixed, then the pendulum just performs linear oscillations in the radial direction.

In new dimensionless variables $z_i(\tau)$, the energy of the oscillating pendulum is given by the following explicit expression:

$$E(\tau) = \frac{1}{18(z_1+1)^2}\begin{pmatrix} -54\,(z_1+1)^3\cos z_2 + 81\,z_1^4 + 162 z_1^3 + \\ \left(81 z_3^2 + 135\right) z_1^2 + \left(162 z_3^2 + 108\right) z_1 + 81\,z_3^2 + 256\,z_4^2 + 54 \end{pmatrix}. \tag{17}$$

Mathematically, the above results represent direct proofs that in our case the modulation theory has more advantages in comparison with numerical investigations. At small and even moderate oscillations, this asymptotic approach allows us to make up a complete parametric analysis of the system under the study. Pragmatically, stability properties demonstrated using the above example of a spring oscillator in post-bifurcation regime can be used when designing an idea of a high-precision angular sensor which can appear in the form of a circular Foucault pendulum, in most simple case, or as a solid-state wave gyro with axisymmetric resonator in more general case (for instance, see [4, 5] and references therein).

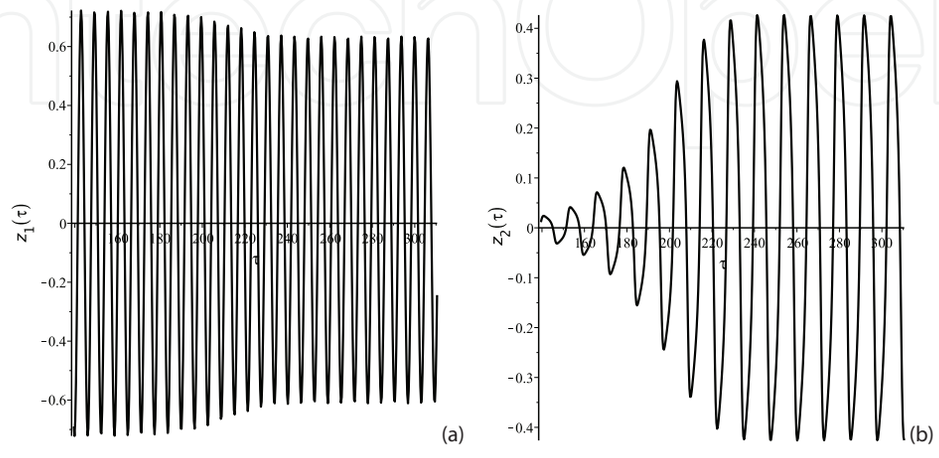

Figure 3. The evolution of the damped forced radial coordinate of the pendulum in time τ (a) and the time history of the resonantly excited angular coordinate of the pendulum in time τ (b).

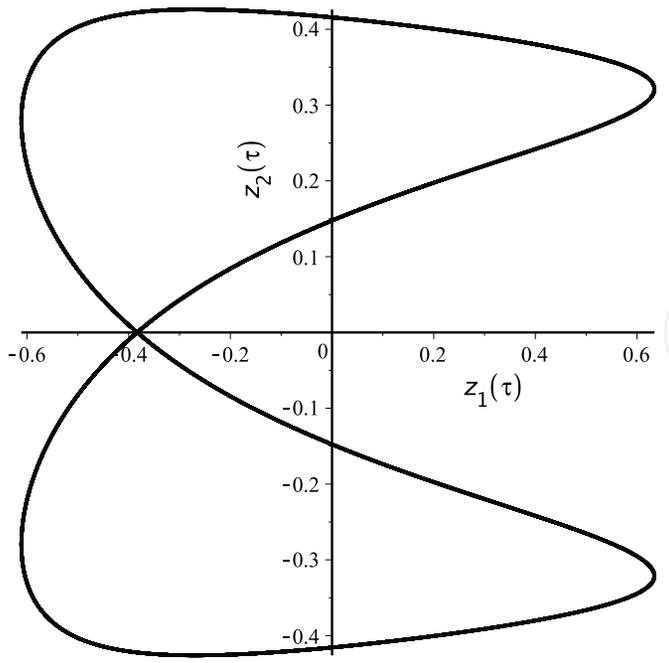

Figure 4. The evolution of the damped forced radial coordinate of the pendulum in time τ.

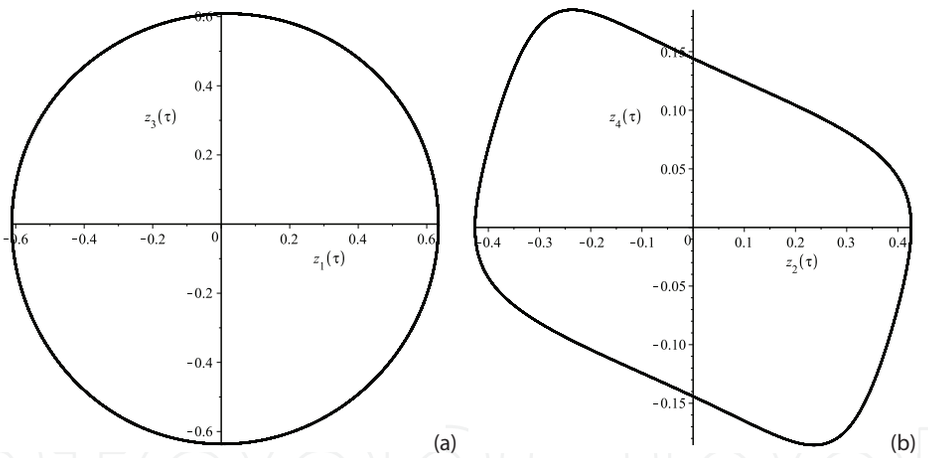

Figure 5. Cross sections of the phase space demonstrating individual dynamical behavior over the radial (a) and angular coordinates (b) at the damped forced oscillations in a spring pendulum in time τ.

Gradually, one may always construct an appropriate theory by further developing the model given by Eq. (1). Nonetheless, here we decided to invoke more general case in our consideration, namely a thin-ring resonator of which is described in detail in [11].

3. Thin-ring resonator

In order to define the in-plane position in a thin-ring resonator, thickness h and radius R, rotating with angular velocity Θ about its sensitive axis, we introduce the two frames of polar

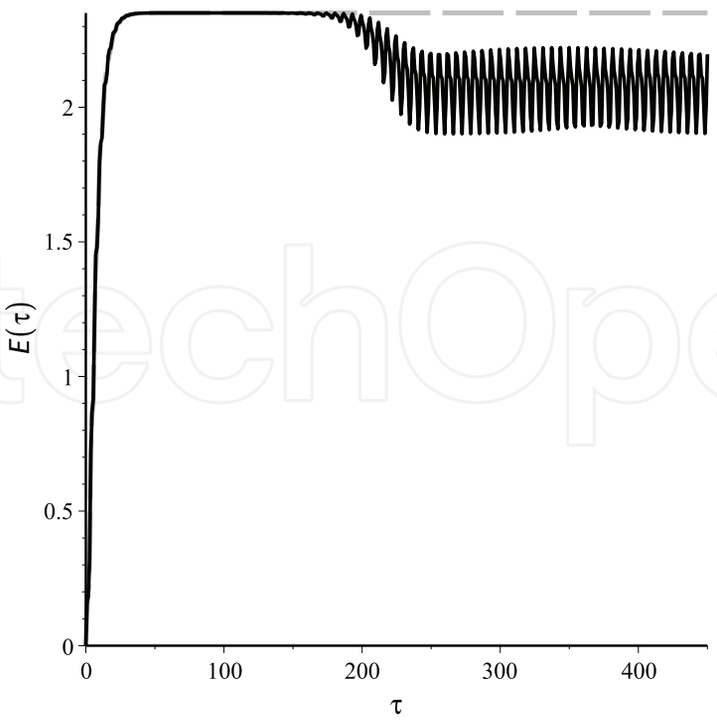

Figure 6. Energy of the pendulum becomes some lower in comparison with the same system with fixed angular coordinate. Dashed line refers to a spring pendulum with constrained to zero angular coordinate.

coordinates in the absolute Newton's space $(R + w, \phi + v/R)$ and in the rotating plane $(R + w, \varphi + v/R)$ where both have the same center as pole. Here, w and v are radial and tangential displacements of the ring, respectively. Therefore, we shall have

$$\phi = \varphi + \Theta t,$$

if the ring rotates uniformly in time t. Also, we may suppose that the angular rate as a slowly varying function of time. In this case, the latter expression is slightly modified by the following integral:

$$\phi = \varphi + \int_{t_0}^{t} \Theta(\tau) d\tau.$$

Equations of motion are derived from the theory of thin-walled shells that uses Kirchhoff-Love hypotheses. So, the field of displacements in the ring is expressed as $u_{(s)} = v - \zeta(w_s - v/R)$ and $u_{(\zeta)} = w$, where $v = v(s,t)$ and $w = w(s,t)$ are the components of displacements, rewritten as functions of the circumferential coordinate s; ζ is the distance from the mid-line along the radius.

In the rotating frame of references, the Lagrangian density of the system reads

$$\mathcal{L} = \frac{\rho F}{2}\left[(v_t + \Theta w + R\Theta)^2 + (w_t - \Theta v)^2\right] - \frac{EF\kappa^2}{2R^2}v^2 - \frac{1}{2}\int_{-h/2}^{h/2} E\epsilon_{ss}^2 d\zeta,$$

where E is Young's modulus; F denotes cross-section square; ρ is mass density; κ characterizes the stiffness of the rotating platform of the ring; $\epsilon_{ss} = v_s + w/R + \xi(w_{s,s} - v_s/R) + w_s^2/2$ is the circumferential component of the deformation tensor. According to paradigms of the variational analysis, equations governing the motion in the ring have the following form:

$$\begin{aligned} &(\mathcal{L}_{\dot{v}})_t + (\mathcal{L}_{v_s})_s - \mathcal{L}_v = Q_{(v)} - \mathcal{R}_{\dot{v}}; \\ &(\mathcal{L}_{\dot{w}})_t + (\mathcal{L}_{w_s})_s - \left(\mathcal{L}_{w_{s,s}}\right)_{s,s} - \mathcal{L}_w = Q_{(w)} - \mathcal{R}_{\dot{w}}, \end{aligned} \tag{18}$$

where $Q_{(v)}$ and $Q_{(w)}$ are introduced as generalized forces; the function $\mathcal{R} = \eta K$, expressed through the kinetic energy K, is respective for the energy dissipation model linearly scaled by the coefficient η. For further preparations, it seems to be continent to rearrange these equations to dimensionless notation:

$$\begin{aligned} &\ddot{v} + 2\mu\Omega\dot{w} + \mu\dot{\Omega}w + \dot{\Omega}/\epsilon - \mu^2\Omega^2 v - V_\varphi + \epsilon^2 W_{\varphi,\varphi} + \kappa^2 v = \frac{\epsilon\mu}{2}\left(w_\varphi^2\right)_\varphi + Q_v; \\ &\ddot{w} - 2\mu\Omega\dot{v} - \mu\dot{\Omega}v - \mu^2\Omega^2 w - \mu\Omega^2/\epsilon + V + \epsilon^2 W_{\varphi,\varphi,\varphi} \\ &\quad = \epsilon\mu\left[\left(Vw_\varphi\right)_\varphi + \frac{w_\varphi^2}{2}\right] + \frac{\epsilon^2\mu^2}{2}\left(w_\varphi^3\right)_\varphi + Q_w, \end{aligned} \tag{19}$$

where $\epsilon = h/\sqrt{12}R \ll 1$ is the relative thickness of the ring; small parameter $\mu = a/R \ll 1$ is intended for making up further procedures of the perturbation analysis; the functions $V = v_\varphi + w$ and $W = w_\varphi - v$ are written for brevity. The transform to these dimensionless variables reads: $v(\tau,\varphi) \to v(s,t)/\mu a$; $w(\tau,\varphi) \to w(s,t)/\mu a$; $\varphi = s/R$; $\tau = tc/R$; $\Omega(\tau) = \Theta(t)R/\mu c$. Here, $c = \sqrt{E/\rho}$ denotes the wave propagation velocity; $a = h/\sqrt{12}$.

Finally, we should provide the set (19) by the periodicity conditions

$$v(\varphi,\tau) = v(\varphi + 2\pi,\tau); \quad w(\varphi,\tau) = w(\varphi + 2\pi,\tau). \tag{20}$$

3.1. Dispersion relation

For studying the wave propagation in the rotating frame of references, it is convenient to define linear modes of oscillations in the ring on the fixed platform. If the rotation is absent, then the normal modes of vibrations represent standing waves being a superposition of two waves traveling toward identical wave numbers, frequencies as well as amplitudes. First of all, we should understand how the spectrum of these oscillatory modes would change in the uniformly rotating ring. Are there the standing modes taking place? And if these cannot be detected, then, what thing should we invoke instead into our study? We know that the precession of waves appears as a reaction on the rotation. Therefore, there will be expected some asymmetry in the polarization vectors of traveling waves. One more finding is we know that the precession rate of waves has to be proportional to the difference between the frequencies in the wave pair as if those compose a standing wave in the ring being at rest. Let the angular rate in the ring be constant and then the wave precession should appear as some sort of kinematic reactions on the rotation of the ring platform. But if the platform rotates with acceleration, then we can expect a kind of some dynamical response that may appear as

essentially differ from kinematic one. Fortunately, experiments with revolving axisymmetric bodies tell us that the expression for the uniformly rotating ring, which will be done subsequently, is equally valid in both cases of the uniformly rotating ring and in the motion with arbitrary, but moderate, angular acceleration [8].

In the case of uniform rotating, a simple solution of the linearized set (19) is given by

$$v(\tau,\varphi) = -\frac{\mu\Omega^2}{\epsilon\left(\mu^2\Omega^2-1\right)} + B\exp i(n\varphi+\omega\tau); \quad w(\tau,\varphi) = A\exp i(n\varphi+\omega\tau),$$

Here, we can trace the appearance of the constant extension in radial direction caused by the centrifuge force. Notice that the amplitudes, A and B, entering therein, are linearly interrelated, that is, $B = pA$, through the interrelation coefficients, p, defined for both the high- and low-frequency sets of normal modes:

$$p_{k,n} = -\frac{i\left(2\mu\Omega\omega_{k,n} + n\left(1+\epsilon^2n^2\right)\right)}{n^2(1+\epsilon^2)+\kappa^2-\left(\omega_{k,n}^2+\mu^2\Omega^2\right)}. \tag{21}$$

The high- and low-frequency branches are indexed by $k = 1$ and $k = 2$, correspondingly. Recall from the linear algebra that these coefficients should satisfy the orthogonality condition, that is, $p_{1,n}p_{2,n} = -1$, for arbitrary wave number n, excluding the one case of linearly decoupled oscillations, taking place at $n = 0$, that is, at axisymmetric radial oscillations. The natural frequencies of waves, $\omega_{k,n}$, are defined by the dispersion relation

$$\left(n^2\left(1+\epsilon^2\right)+\kappa^2-\left(\omega^2+\mu^2\Omega^2\right)\right)\left(1+\epsilon^2n^4-\left(\omega^2+\mu^2\Omega^2\right)\right)-\left(2\mu\Omega\omega-n\left(1+\epsilon^2n^2\right)\right)^2=0. \tag{22}$$

Let the angular velocity be zero and then the dispersion relation turns into the simple algebraic equation

$$-n^6\epsilon^2-\epsilon^2\left(-\omega^2-2+\kappa^2\right)n^4+\left(\left(\omega^2-1\right)\epsilon^2+\omega^2\right)n^2-\omega^4+\left(1+\kappa^2\right)\omega^2-\kappa^2=0, \tag{23}$$

Two identical ones of all the four roots of Eq. (23) are shown in **Figure 7**. The low-frequency branch refers in general to the bending modes while the high-frequency ones reply mainly to the circumferential modes of extension.

In the case of a small angular rate, that is, $\Omega \ll \omega_{k,n}$, the roots of the dispersion relation (22) are approximately represented as follows:

$$\omega_{k,n}(\Omega) \approx \omega_{k,n}(0) + \frac{2\mu\Omega n\left(1+\epsilon^2n^2\right)}{1+\epsilon^2n^4+(1+\epsilon^2)n^2+\kappa^2-2\left(\omega_{k,n}(0)\right)^2}. \tag{24}$$

It may not, perhaps, be out of place to note that these roots possess by asymmetry because of the angular rate. Nonetheless, each frequency, $\omega_{k,n}$, can be decomposed on the antisymmetric term as well as on the symmetric part. The antisymmetric term is respective for the wave precession caused by the ring rotation while the symmetric one describes a small inessential correction.

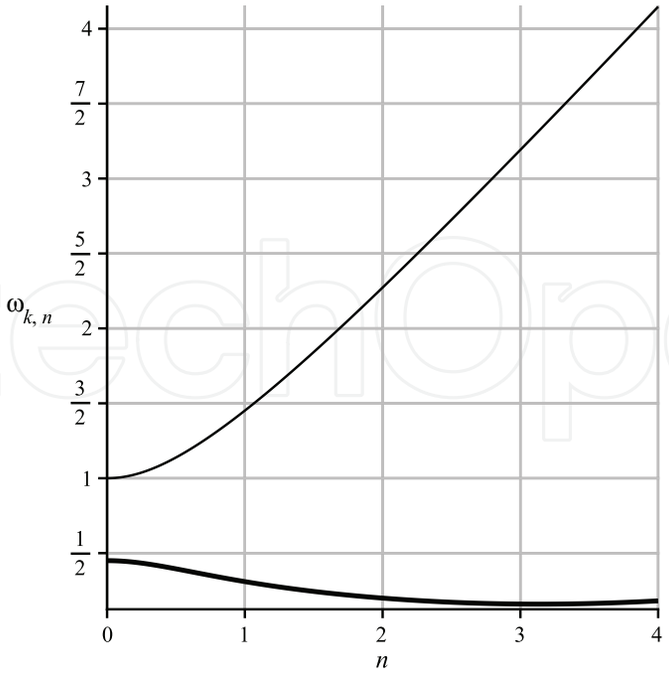

Figure 7. The high- and low-frequency dispersion branches for waves on the fixed platform ($\epsilon = 0.01$, $\kappa = 0.45$, $\Omega = 0$).

4. Nonlinear resonant coupling between the axisymmetric radial oscillation and two similar bending wave forms being in phase

This section invokes briefly some general points from the common theory of waves, including understanding phenomena of resonance experienced in nonlinear mechanical systems and some mathematical preparations which are necessary to investigate the given problem from the viewpoint of the perturbation analysis, using methods of slowly varying amplitudes and phases. Then, we generalize the problem by considering the case of damped forced oscillations in a thin circular ring. This generalization of the problem leads to a thought on how to excite stable wave precession regimes which need no feedback to repair unwanted motions in the solid-state wave gyro.

4.1. Triple-mode resonant coupling between waves in the ring

Truncated equations or evolution equations describing the modulation phenomena of amplitudes and phases can be directly obtained using the following anzats [12–15]:

$$v(\tau,\varphi) = \sum_{k=1}^{3} p_k A_k(T)\exp i\phi_k; \quad w(\tau,\varphi) = \sum_{k=1}^{3} A_k(T)\exp i\phi_k, \tag{25}$$

which represent an approximated solution to Eq. (19). Here, $A_k(T)$ $(k = 1..3)$ are the slowly varying complex wave amplitudes, evolving at slow time $T = \mu\tau$; $\phi_1 = n\varphi + \omega_1\tau$, $\phi_2 = -n\varphi + \omega_1\tau$, $\phi_3 = \omega_3\tau$ are the fast rotating phases; $(^*)$ denote the complex conjugation. Notice that the amplitude and phase number three refer to the axisymmetric radial oscillation of the ring.

We assume that the angular rate and acceleration of the ring are small enough, that is, $\Theta(\tau) \sim \mu$ and $d\Theta/d\tau \sim \mu^2$. Also, we should suppose that spectral parameters of waves in the solution (25) are matched by the following phase synchronicity conditions:

$$\omega_3 = \omega_1 + \omega_2 + \mu\Delta\omega, \tag{26}$$

where $\Delta\omega$ denotes a small discrepancy between the phases of the high-frequency axisymmetric radial oscillation and two low-frequency quasi-harmonic waves with amplitudes, numbers one and two. Certainly, all the frequencies ω_1, ω_2, ω_3 and the wave numbers $\pm n$ should satisfy the dispersion relation (23). In the theory of nonlinear waves, such a trio is used to name a *resonant triplet* while the synchronicity (26) is associated with the so-called *phase-matching conditions*.

One more convenient way of obtaining the evolution equation is walking down along the Hamiltonian formalism. Let us consider the average Lagrangian of the system

$$\langle\mathcal{L}\rangle = \left(\frac{1}{2\pi}\right)^3 \int_0^{2\pi}\left(\int_0^{2\pi}\left(\int_0^{2\pi}\mathcal{L}d\phi_1\right)d\phi_2\right)d\phi_3, \tag{27}$$

in order than to expand this one in a formal series in small parameter μ as follows:

$$\langle\mathcal{L}\rangle = \mathcal{L}_0 + \mu\mathcal{L}_1 + \mu^2\mathcal{L}_2 + \ldots,$$

Here, zero-order approximation term, that is, $\mathcal{L}_0 = 0$, would coincide exactly with the dispersion relation, accordingly to findings of Whitham [16]. The second term $\mathcal{L}_1$, entering this expansion, describes effects arising in the first-order nonlinear approximation analysis which we need to study here. Then, the nontrivial average Hamiltonian of the system would read

$$\mathcal{H} = \sum_{k=1}^{3}\left(A_{k,T}\frac{\partial\mathcal{L}_1}{\partial A_{k,T}} + \overline{A}_{k,T}\frac{\partial\mathcal{L}_1}{\partial\overline{A}_{k,T}}\right) - \mathcal{L}_1,$$

In this case of resonant coupling between the axisymmetric radial oscillation and two low-frequency bending waves, being in phase (26), this average Hamiltonian is rearranged in more pragmatic form

$$\mathcal{H} = 2i\Omega\sum_{j=1}^{2}\omega_j\left(\overline{p_j} - p_j\right)\left|A_j\right|^2 + \epsilon n^2\left[\overline{A}_1\overline{A}_2A_3\exp\left(i\Delta\omega T\right) + A_1A_2\overline{A}_3\exp\left(-i\Delta\omega T\right)\right]. \tag{28}$$

Recall that the bending wave frequency $\omega = \omega_1 = \omega_2$ should be close to the frequency $\omega_3/2$ that denotes the frequency of the axisymmetric radial oscillation, that is, $\omega_3 = 1$. Note that the case under consideration is associated with the *principal parametric resonance*. His Hamiltonian produces a set of following evolution equations:

$$\begin{aligned}
\frac{dA_1}{dT} &= \frac{2\Omega\left(\overline{p_1} - p_1\right)}{1+p^2}A_1 - \frac{i\epsilon n^2}{\omega(1+p^2)}\overline{A}_2A_3\mathrm{e}^{i\Delta\omega T}\\
\frac{dA_2}{dT} &= \frac{2\Omega\left(\overline{p_2} - p_2\right)}{1+p^2}A_1 - \frac{i\epsilon n^2}{\omega(1+p^2)}\overline{A}_1A_3\mathrm{e}^{i\Delta\omega T};\\
\frac{dA_3}{dT} &= -i\epsilon n^2A_1A_2\mathrm{e}^{-i\Delta\omega T},
\end{aligned} \tag{29}$$

where $p_k = (-1)^k in\left(1+\epsilon^2 n^2\right)/\left(\left(1+\epsilon^2\right)n^2-\omega^2\right)$ are the wave polarization coefficients which satisfy the equality $p = |p_1| = |p_2|$, due to the symmetry of the problem.

Now, we use the following transform of variables:

$$\begin{aligned} A_1 &= a_1 \exp\left(\frac{2\left(\overline{p_1}-p_1\right)}{1+p^2}\int_0^T \Omega(\varsigma)d\varsigma\right); \\ A_2 &= a_2 \exp\left(\frac{2\left(\overline{p_2}-p_2\right)}{1+p^2}\int_0^T \Omega(\varsigma)d\varsigma\right); \\ A_3 &= a_3, \end{aligned} \tag{30}$$

that allows us to rewrite the set (29) by getting rid of Coriolis terms:

$$\begin{aligned} \frac{da_1}{dT} &= -\frac{i\epsilon n^2}{\omega(1+p^2)}\overline{a}_2 a_3 e^{i\Delta\omega T}; \\ \frac{da_2}{dT} &= -\frac{i\epsilon n^2}{\omega(1+p^2)}\overline{a}_1 a_3 e^{i\Delta\omega T}; \\ \frac{da_3}{dT} &= -i\epsilon n^2 a_1 a_2 e^{-i\Delta\omega T}, \end{aligned} \tag{31}$$

Eq. (32) have now obtained a standard form similar to Euler's kinematic equations describing rotation of a rigid body with a fixed point. This set can be integrated exactly in terms of the Jacobi elliptic functions [17]. Also, here is a place to note that in the theory of nonlinear waves similar equations describe *break-up instability* phenomena when the high-frequency mode becomes unstable triad with respect to small low-frequency perturbations [12].

4.2. Resonant excitation of the gyro

Let us invite in our consideration the generalized forces describing the damping and forcing of the ring resonator over the axisymmetric form of oscillation. By substituting the terms $Q_v = -2\mu\eta\dot{v}$; and $Q_w = -2\mu(\eta\dot{w} - Q\cos\varpi\tau)$ into Eq. (19), we can obtain, after the exchange of variables (30), the following set of evolution equations:

$$\begin{aligned} \frac{da_1}{dT} &= -\eta a_1 - \frac{i\epsilon n^2}{\omega(1+p^2)}\overline{a}_2 a_3 e^{i\Delta\omega T}; \\ \frac{da_2}{dT} &= -\eta a_2 - \frac{i\epsilon n^2}{\omega(1+p^2)}\overline{a}_1 a_3 e^{i\Delta\omega T}; \\ \frac{da_3}{dT} &= -\eta a_3 + iQe^{i\delta T}/2 - i\epsilon n^2 a_1 a_2 e^{-i\Delta\omega T}, \end{aligned} \tag{32}$$

that can be rewritten, after one more exchange of variables; $a_j(T) = b_j(T)e^{i\varphi_j(T)}$, in terms of real-valued amplitudes and phases:

http://dx.doi.org/10.5772/intechopen.71726

$$\begin{aligned}
&\frac{db_1}{dT} = -\eta b_1 + \frac{\epsilon n^2 b_2 b_3 \sin\psi}{\omega(1+p^2)};\\
&\frac{db_2}{dT} = -\eta b_2 + \frac{\epsilon n^2 b_1 b_3 \sin\psi}{\omega(1+p^2)};\\
&\frac{db_3}{dT} = -\eta b_3 - \epsilon n^2 b_1 b_2 \sin\psi + Q\sin(\delta T - \varphi_3)/2;\\
&\frac{d\psi}{dT} = -\Delta\omega + \frac{-2n^2\epsilon\left(b_1^2\left(\omega\left(1+p^2\right)b_2^2 - b_3^2\right) - b_2^2 b_3^2\right)\cos\psi + \omega b_1 b_2 Q\cos(\delta T - \varphi_3)\left(1+p^2\right)}{2\omega(1+p^2)b_1 b_2 b_3};\\
&\frac{d\varphi_3}{dT} = -\epsilon n^2 b_1 b_2 \cos\psi/b_3 + Q\cos(\delta T - \varphi_3)/2b_3,
\end{aligned} \tag{33}$$

where $\psi(T) = \varphi_3(T) - \varphi_2(T) - \varphi_1(T) + \Delta\omega T$. These equations are convenient in the study of stationary damped forced motions performed in the system (32). There are two subsets of such motions; the first can be written as

$$b_1 = b_2 = 0; \quad b_3 = \frac{K\left(1+p^2\right)\eta\omega}{\epsilon n^2}, \tag{34}$$

while the second would be

$$b_1 = b_2 = \frac{\sqrt{2}\eta\omega\sqrt{1+p^2}\sqrt{K-1}}{\epsilon n^2}; \quad b_3 = \frac{\eta\omega\left(1+p^2\right)}{\epsilon n^2}. \tag{35}$$

Here, we have introduced a new notation: $K = Qn^2\epsilon/\left(4\left(1+p^2\right)\eta^2\omega^2\right)$ for the characteristic number by analogy with Reynolds numbers in the hydrodynamics [18, 19].

Now, we may return to our preliminary study over the spring pendulum to be acquainted in similarities and analogies. Indeed, the first stationary solution (34) appears as stable only within the range $0 \le K \le K^*$. Here, $K^* = 1$ denotes the critical value of the control parameter governing the bifurcations. This stationary solution coincides exactly with the solution if neglecting all the nonlinear terms in the system (19). Although near the point K^* this stationary solution loses its stability to give its place for the new stationary state (35). The new stationary state would be stable at $K > 1$. It is not now surprising that as if the bifurcation parameter K grows even further, then the energy would be pumped only into the low-frequency bending modes while the amplitude of the high-frequency axisymmetric radial mode remains to be fixed, that is, $b_3 = \eta\omega\left(1+p^2\right)/\left(\epsilon n^2\right)$. Probably, this mechanism represents an effective way in the problem of installation of the solid-state wave gyro.

When returning to the old notation, the solution of our problem can be expressed as it follows:

$$\begin{aligned}
v(\tau,\varphi) &= -4pb_1\cos(\psi(\tau) - n\varphi)\cos\left(\omega + \mu\left(\frac{\delta+\Delta\omega}{2}\right)\right)\tau + O\left(\mu^2\tau\right);\\
w(\tau,\varphi) &= -4b_1\sin(\psi(\tau) - n\varphi)\cos\left(\omega + \mu\left(\frac{\delta+\Delta\omega}{2}\right)\right)\tau - 2b_3\sin(\varpi\tau) + O\left(\mu^2\tau\right),
\end{aligned} \tag{36}$$

where

$$\psi(\tau) = \frac{4p}{1+p^2}\int_0^{\tau} \Omega(\varsigma)d\varsigma$$

is the precession rate. Typical patterns of the wave precession are shown in **Figure 8**.

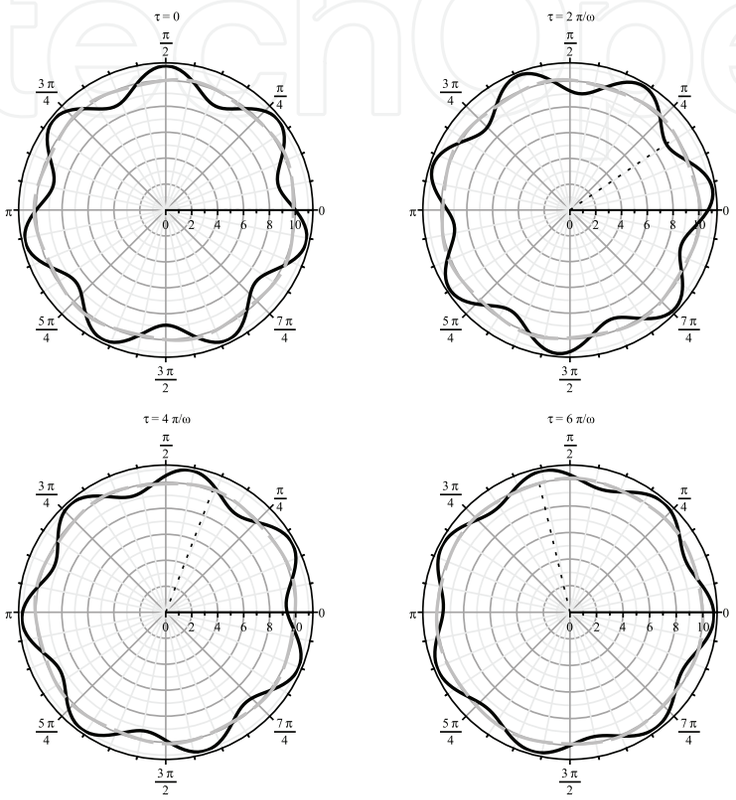

Figure 8. The wave precession. Modal number $n = 7$. Solid lines refer to flexural mode, while the dashes to the circumferential one ($\eta = 0.1$, $\mu = \epsilon \approx 0.01$, $\kappa = 0.45, \Omega = 0.085$, Q = 0.1). The dotted radius indicates the rotation angle $\Omega\tau$. The stiffness of the gyro platform κ is tuned to the seventh bending modes.

5. Conclusion

Léon Foucault has made a sensation with his famous giant pendulum experiment in the Panthéon in Paris in 1851. That time, people could perceive the inertia of the pendulum with his naked eye to have the first direct proof that the Earth is turning anti-clockwise. Moreover, this experiment has demonstrated that a pendulum could be used as a vibratory gyro. However, a flaw of the Foucault pendulum is the dependence on the latitude. A device was needed that was unaffected by the latitude. In 1852, Foucault proposed an angular sensor based on the immobility of the axis of a rotating mass. Unlike the pendulum, this sensor could detect a fixed direction in Newton's absolute space. Recall that a torque directing the axis of rotation of the rotor of the gyro is known as the precession. For the precision, however, this gyro required an exquisite construction, since the gyro's rotor should be balanced as well as possible.

In 1890, Bryan investigated the nature of the beats which may be heard when a vibrating cylinder or other axisymmetric thin-walled shell of revolution has been involved in a rotatory motion about its axis [7]. Perhaps, this study had been inspired as a reply to A. E. H. Love, famous for his work on the mathematical theory of elasticity. In the paper [20], Love supposed that unless a body was revolving with the angular velocity comparable with the frequencies of the vibrations, the latter would not be almost affected. The only important effect of rotation would be an extension because of the centrifugal force. Bryan has corrected that in the axisymmetric shells at high-frequency vibrations phenomena of beats may be observed, which appears as the most noticeable effects of the rotation. It is probable that Bryan had no idea how to utilize his finding. Though those times people were in controversy on how far theory of thin-walled shells elaborated by Lord Rayleigh is capable of practice, is this perhaps just a sort of one more abstract theory? Lo and behold, initially conceived in 1890 through the observation of beats from a ringing wine glass, the concept was lost until uncovered in 1965. Due to technologies of the second half of the twentieth century, perhaps in times of Vietnam War, this physical effect has inspired a concept of a solid-state wave gyro [6]. Because there are no typical mechanical parts, these wave sensors have a lot of advantages for long-term space missions. However, to maintain the functionality as well as the sensitivity of a conventional wave gyro in practice, the driving of standing waves requires somewhat sophisticated feedback control. This chapter demonstrates that when both the primary resonant pumping over the axisymmetric mode of oscillations and advantages of the principal parametric resonance are combined, such a gyro can operate without any feedback at the expense of the natural nonlinearity of the resonator in a post-bifurcation regime.

Author details

Svetlana Pavlovna Nikitenkova[1]* and Dmitry Anatolyevich Kovriguine[2]

*Address all correspondence to: spnikitenkova@gmail.com

1 Radiophysics Faculty, Nizhny Novgorod State University n.a. N.I. Lobachevsky, Nizhny Novgorod, Russia

2 Applied Mathematics Chair, Nizhny Novgorod Technical State University n.a. R.E. Alekseev, Nizhny Novgorod, Russia

References

[1] https://www.grc.nasa.gov/www/K-12/airplane/dragsphere.html (Drag of a Sphere - NASA)

[2] Lee J. Triad-angle locking in low-order models of the 2D Navier-Stokes equations. Physica D: Nonlinear Phenomena. 1987;**24**(1–3):54-70

[3] Sukhorukov AP. Nonlinear Wave Interactions in Optics and Radio Physics. Moscow: Nauka; 1988

[4] Zhuravlev VF. Global evolution of state of the generalized Foucault pendulum. Mechanics of Solids. 1998;**33**(6):1-6

[5] Stanovnik A, Jurčič-Zlobec B. Numerical study of the elastic pendulum on the rotating earth. ISRN Mathematical Physics. 2012, Article ID 806231;**2012**:1-7

[6] Lynch DD. HRG Development at Delco, Litton, and Northrop Grumman. Proc. of Anniversary Workshop on Solid-State Gyroscopy (19–21 May 2008. Yalta, Ukraine). Kyiv-Kharkiv. ATS of Ukraine, ISBN 978–976–0-25248-5; 2009

[7] Bryan GH. On the beats in the vibrations of a revolving cylinder or bell. Proceedings of Cambridge Philosophical Society of Mathematics and Physical Sciences. 1890;**VII**(III):101-111

[8] Zhuravlev VF, Klimov DM. Wave Solid-State Gyro. Moscow: Nauka Publisher; 1985 (in Russian)

[9] Bose A, Puri S, Banerjee P. Modern Inertial Sensors and Systems. Prentice-Hall of India: New Delhi, II; 2008

[10] Osiander R, Ann Garrison Darrin M, Champion JL. MEMS and Microstructures in Aerospace Applications. Taylor & Francis Publisher. ISBN 0824726375; 2005

[11] Kovriguine DA. Geometrical nonlinearity stabilizes a wave solid-state gyro. Archive of Applied Mechanics. 2014;**84**(2):159-172

[12] Phillips OM. The dynamics of the upper ocean. Cambridge Univ. Press; 1977

[13] Kovriguine DA, Potapov AI. Nonlinear oscillations in a thin ring - I, II. Acta Mechanica. 1998;**126**:189-212

[14] Kovriguine DA. On non-linear resonant excitation of a wave solid-state gyro. Proc. of Int. Cong. MV2 New advances in modal synthesis of large structures, non-linear, damped and non-deterministic cases, Jezequel Ed., École Centrale de Lyon. 1995;**2**:575-586

[15] Kovriguine DA. Geometrical nonlinearity stabilizes a wave solid-state gyro. Archive of Applied Mechanics. 2014;**84**(2):159-172

[16] Whitham GB. Linear and Nonlinear Waves. New-York: Wiley-Interscience; 1995

[17] Janke-Emde-Lösch: Tafeln Höherer Funktionen. Sechste auflage. Neubearbeitet von F. Lösch, B.G.Teubuer, Verlagsgesellschaft. Stuttgard. 1960

[18] Gledzer EB, Dolzhansky FW, Obukhov AM. Systems of hydrodynamic type and their applications. Moscow: Nauka Publisher; 1981 (in Russian)

[19] Nayfeh A, Balachandran B. Applied Nonlinear Dynamics: Analytical. New-York: Computational and Experimental Methods. Wiley; 1995

[20] Love AEH. The free and forced vibrations of an elastic spherical shell containing a given mass of liquid. Proceedings of the London Mathematical Society. 1887;**1**(1):170-207